

Cascade hypernuclear production spectra at J-PARC

Hideki Maekawa, Kohsuke Tsubakihara, Hiroshi Matsumiya and Akira Ohnishi

Department of Physics, Faculty of Science, Hokkaido University Sapporo 060-0810, Japan

Abstract

We predict cascade hypernuclear production spectra expected in the forthcoming J-PARC experiment. In the Green's function method of the distorted wave impulse wave approximation with the local optimal Fermi averaging t -matrix, we can describe the Ξ^- production spectra in the continuum and bound state region reasonably well. Predictions to the high resolution spectra at J-PARC suggest that we should observe Ξ^- bound state peak structure in (K^-, K^+) spectra in light nuclear targets such as ^{12}C and ^{27}Al .

Key words: Ξ Hypernuclei, Distorted wave impulse approximation, Fermi averaging

PACS: 21.80.+aHypernuclei and 24.50.+gDirect reactions

1. Introduction

Investigation of nuclear systems with strangeness opens up a way to understand dense matter such as the neutron star core. Since strange quarks are negatively charged and cancel the positive proton charge, they are favored in charge neutral dense matter. As a result, many models predict hyperons would appear at around $2\rho_0$, and Λ may share a similar or larger fraction to neutrons at very high densities.

In describing highly dense matter, we clearly need information on BB interaction not only for $S = 0, -1$ but also for $S \leq -2$ such as ΞN , but spectroscopic information on cascade (Ξ) hypernuclear systems are severely limited at present. While old emulsion data suggest a deep Ξ^- -nucleus potential (~ -24 MeV) [1], a shallow potential (~ -15 MeV) is suggested from the twin hypernuclear event found in a nuclear emulsion [2]. This shallow potential is also supported by the distorted wave impulse approximation (DWIA) analysis of Ξ^- production spectra in the bound state region [3,4].

In order to extract as much information as possible from the data available at present, we need to investigate the Ξ^- hypernuclear production spec-

tra by (K^-, K^+) reaction on nuclear targets in both of the *continuum* as well as the bound state region. Since the DWIA analysis in [4] strongly rely on the absolute value of the inclusive Ξ^- production yield, it is necessary to verify the consistency with the production spectra in the quasi free (QF) region [5]. For this purpose, the Green's function method of DWIA would be a useful tool, where the continuum and bound state spectra can be described on the same footing.

In this paper, we investigate the Ξ^- -nucleus potential through Ξ^- production spectra in the continuum and bound state region in the Green's function method of DWIA with the local optimal Fermi averaging t -matrix (LOFAt), in which the Ξ^- -nucleus potential effects are included in both of the strength function and the transition amplitude. Based on the analyses of the observed continuum and bound region spectra, we make predictions to the future coming Ξ^- hypernuclear production experiment at J-PARC. We find that we should observe Ξ^- hypernuclear bound state peak structures in (K^-, K^+) spectra on light nuclear targets such as ^{12}C and ^{27}Al as far as the imaginary part of the Ξ^- -nucleus optical potential is not large ($|W_{\Xi}| \leq 3$ MeV) and the exper-

imental resolution is good enough ($\Delta E \leq 2$ MeV).

2. Green's function method and Local optimal Fermi averaging t -matrix

The Green's function method in DWIA has been widely applied to analyse hypernuclear reactions. This method has an advantage that we can describe the continuum as well as bound state region on the same footing. In DWIA, the differential cross section reaction is obtained from the Fermi's golden rule [6], and the response function $R(E)$ can be decomposed into multipole components in the Green's function method [7],

$$\frac{d^2\sigma}{dE_{K^+}d\Omega_{K^+}} = \frac{p_{K^+}E_{K^+}}{(2\pi\hbar^2)^2v_{K^-}}R(E), \quad (1)$$

$$R(E) = \sum_f |\mathcal{T}_{fi}|^2 \delta(E_f - E_i), \quad (2)$$

$$= \sum_{JM\alpha\beta\alpha'\beta'} W[\alpha\beta\alpha'\beta'] R_{\alpha\beta\alpha'\beta'}^{JM}(E),$$

$$R_{\alpha\beta\alpha'\beta'}^{JM}(E) = -\frac{1}{\pi} \text{Im} \int r^2 dr r'^2 dr' \bar{t}^*(r) \bar{t}(r') \times f_{JM\alpha}^*(r) G_{\alpha\beta\alpha'\beta'}^{JM}(E; r, r') f_{JM\alpha'}(r'), \quad (3)$$

$$f_{JM\alpha}(r) = \tilde{j}_{JM}(r) \phi_\alpha(r), \quad (4)$$

$$W[\alpha\beta\alpha'\beta'] = (j_N \frac{1}{2} J_0 |j_Y \frac{1}{2}) (j'_N \frac{1}{2} J_0 |j'_Y \frac{1}{2}) \times \delta_{l'_N+l_Y+J}^E \delta_{l'_N+l'_Y+J}^E \sqrt{(2j_N+1)(2j'_N+1)}. \quad (5)$$

where v_{K^-} is the incident K^- velocity, subscripts α and β stand for the quantum numbers of nucleon and hyperon states, respectively, J is the total spin of hypernuclei, $\delta_n^E = 1$ and 0 for even and odd n , and $\phi_\alpha(r)$ is the radial wave function of the target nucleon. Dependence on the Ξ^- -nucleus optical potential U_Ξ appears through the Green's function $G_{\alpha\beta\alpha'\beta'}(E; r, r')$, which contains the hypernuclear Hamiltonian. The function \tilde{j}_{JM} is a radial part of the product of distorted waves $\chi_{K^+}^{(-)*} \chi_{K^-}^{(+)}$ evaluated in the eikonal approximation. We employ the $t\rho$ approximation for the imaginary part of distortion potential, $\text{Im}U_K(r) = \hbar v_K \bar{\sigma}_{KN} \rho(r)$, where $\bar{\sigma}_{KN}$ is the isospin averaged cross sections with $\bar{\sigma}_{NK^-} = 28.90$ mb and $\bar{\sigma}_{NK^+} = 19.35$ mb at $P_{K^-} = 1.65$ GeV/c. For the real part, we adjust its strength to reproduce the total cross section data of K mesons [8]. The elementary t -matrix elements are usually assumed to be independent from the reaction point, and the Fermi averaging t -matrix squared are factorized [9].

For Λ and Σ productions, it is recently pointed out that on-shell kinematics in the Fermi averaging (optimal Fermi averaging, OFA) procedure roughly decide the shape of the QF spectrum [11] in the Green's function method with factorized t -matrix, and similar procedure for t -matrix was proposed in Ref. [12]. In the Semi Classical Distorted Wave (SCDW) analyses [13], the local Fermi averaging of the elementary cross section has been included. Here we would like to incorporate both of the above two ideas; we include the local optimal Fermi averaging t -matrix (LOFAT), $\bar{t}(r)$, in the integrand of the response function Eq. (3). We define the LOFAT as,

$$\bar{t}(r; \omega, \mathbf{q}) \equiv \frac{\int d\mathbf{p}_N t(s, t) \rho(p_N) \delta^4(P_f^\mu(r) - P_i^\mu(r))}{\int d\mathbf{p}_N \rho(p_N) \delta^4(P_f^\mu(r) - P_i^\mu(r))}, \quad (6)$$

where $P_{i,f}^\mu(r)$ denote the four total momenta in the elementary initial and final two-body states. We adopt the Fermi distribution function for the target nucleon momentum distribution $\rho(p_N)$ and parameters are taken from [6,10]. In obtaining LOFAT, we define the i -th hadron single particle energy containing the nuclear and hypernuclear potential effects as,

$$E_i(r) = \sqrt{\mathbf{p}_i^2 + m_i^2 + 2m_i V_i(r)} \sim m_i + \frac{\mathbf{p}_i^2}{2m_i} + V_i(r). \quad (7)$$

This treatment enables us to include the potential effects naturally through the effective mass $m_i^{*2} = m_i^2 + 2m_i V_i(r)$, as adopted in transport models in high-energy heavy-ion collisions [14]. Consequently, the LOFAT has the dependence on the collision point r through hadron potentials $V_i(r)$.

3. Results

In the calculation, we have assumed the one body Woods-Saxon type hyperon-nucleus optical potential, $U_\Xi(r) = (V_0^\Xi + iW_0^\Xi) f(r) + V_C^\Xi(r)$, with $f(r) = 1/(1+\exp((r-R)/d))$, $R = r_0(A-1)^{1/3}$, $d = 0.65$ fm, $r_0 = 1.1$ fm, where $V_C^\Xi(r)$ denotes Ξ^- -core nucleus Coulomb potential. We assume the imaginary part of optical potential W_0^Ξ to be -1 MeV, which simulates the strength in the quark cluster model and the Nijmegen potential model D [15] estimations. We have adopted the elementary t -matrix, which is re-parameterized to fit the cross section and angle dependence for $P_{K^-} \lesssim 3$ GeV/c.

Figure 1 shows the calculated results of Ξ^- QF production spectra with potential depth of 14 MeV

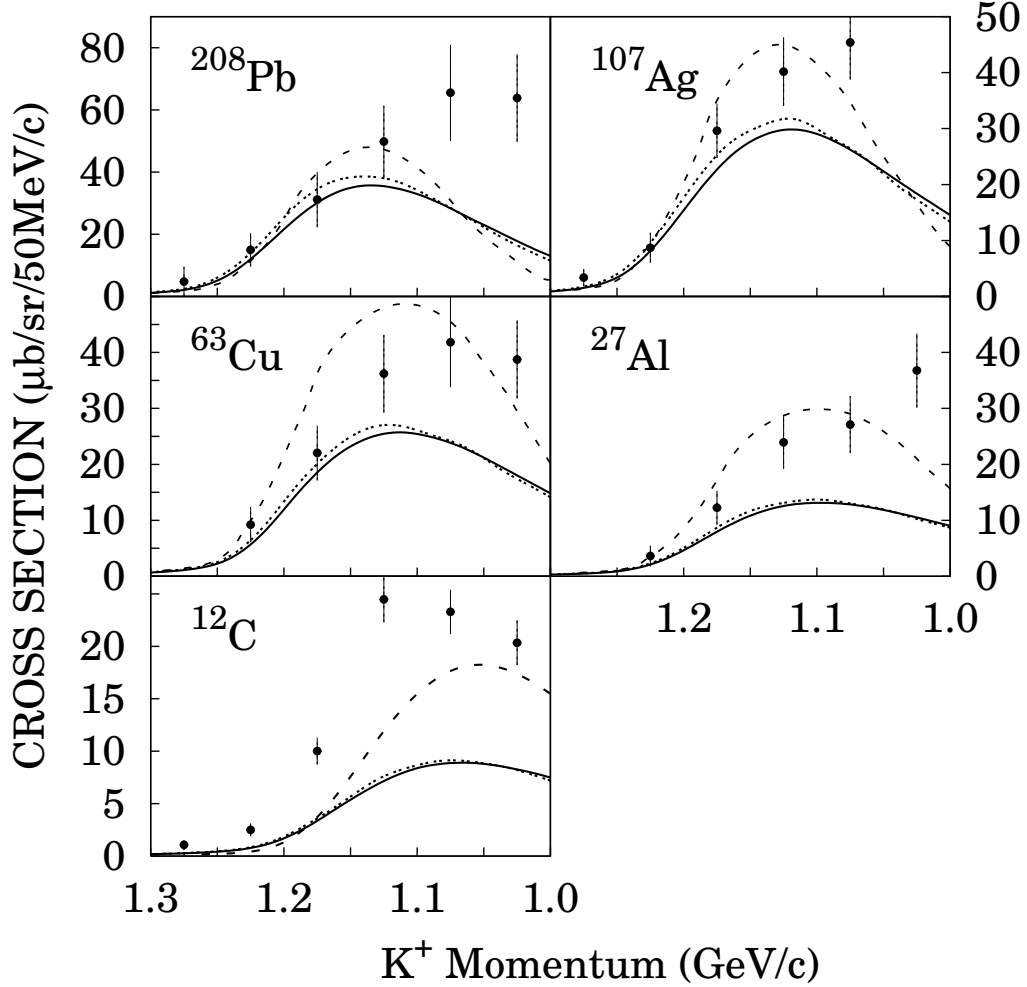


Fig. 1. Calculated Ξ^- -hypernuclear production spectra in the QF region at $p_{K^-} = 1.65$ GeV/c and $\theta_{K^+} = 6$ deg. on C, Al, Cu, Ag and Pb targets in comparison with data [5]. Solid lines show LOFAt + DWIA results with $(V_0^{\Xi}, W_0^{\Xi}) = (-14\text{MeV}, -1\text{MeV})$, and dotted lines show the results without Kaon potential effects. In both of the calculations, the experimental resolution is assumed to be $\Delta E = 20$ MeV (FWHM).

in comparison with experimental data [5]. Calculated curves reproduce the experimental data systematically on heavy targets, Cu, Ag, and Pb, in the high p_{K^+} region, where the hypernuclear excitation is small. In the lower p_{K^+} region, other contributions have been known to be important [16,17], including heavy-meson production and its decay, $K^-N \rightarrow MY, M \rightarrow K^+K^-$ ($M = \phi, a_0, f_0$) [16] and the two-step strangeness exchange and production processes, $K^-N \rightarrow MY, MN \rightarrow K^+Y$ ($M =$

π, η, ρ, \dots) [17].

We underestimate the production spectra on lighter targets, ^{12}C and ^{27}Al . The underestimate of QF spectrum on ^{12}C target is a common feature in previous DWIA calculations [9,18]. In Ref. [13], it is discussed that this underestimate may be due to the center-of-mass effects: For electron scattering on a nucleus with mass number A , the center-of-mass correction in the shell model have been taken care of by a multiplicative factor $F^{1/2} =$

$\exp[q^2/(4m_N A \hbar \omega)]$ for the form factor, where q is the momentum transfer. With $\hbar \omega = 41A^{-1/3} \text{MeV}$, the factor $[F^{1/2}]^2$ amounts to 1.86, 1.43, 1.22, 1.16 and 1.10 for ^{12}C , ^{27}Al , ^{63}Cu , ^{109}Ag and ^{208}Pb targets, respectively, at $q = 500 \text{ MeV}/c$. In Ref. [19], we have adopted a different elementary t -matrix parameterization [17] and larger isospin-averaged KN cross sections, then we can roughly explain the target mass dependence, as shown with the dashed lines in Fig. 1.

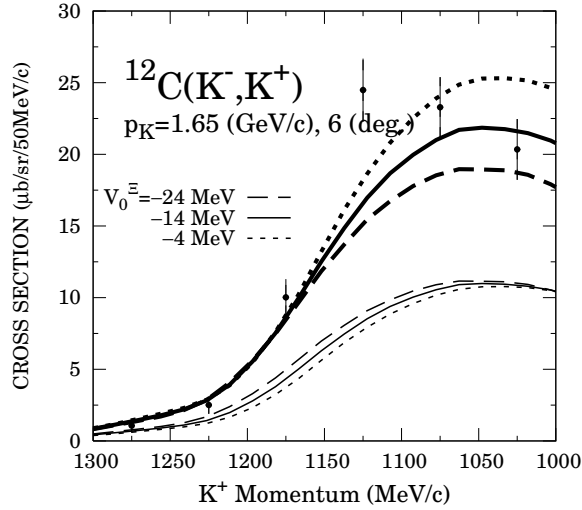


Fig. 2. Calculated Ξ^- production spectra on ^{12}C target at $P_{K^-} = 1.65 \text{ (GeV/c)}$, 6 (deg.) . Calculated curves are shown for the potential depth of -24 MeV (dotted), -14 MeV (solid) and -4 MeV (dashed). Thick lines show the results with multiplicative factors (1.7, 1.99 and 2.35 for $V_0^- = -24, -14, -4 \text{ MeV}$, respectively) introduced to fit the data, and thin lines show calculated results without these factors.

Since our understanding is not complete and we have several ambiguities described above for the absolute yield in QF spectra, we introduce an adjustable multiplicative factor to fit the QF spectrum at low excitation energies (high K^+ momentum region). In Fig. 2, we show the calculated Ξ^- production spectra with Ξ^- potential depth of $V_0^- = -24, -14$ and -4 MeV with multiplicative factors in comparison with data [5]. The potential depth dependence is small in low p_{K^+} region, and attractive potential shifts the spectrum towards the high p_{K^+} direction slightly. When we adjust the multiplication factors as described above, calculated results reasonably well explain the QF spectrum. This means that we cannot determine the potential depth accurately from the QF spectrum shape.

On the other hand, production spectrum is more sensitive to the potential depth at low excitation en-

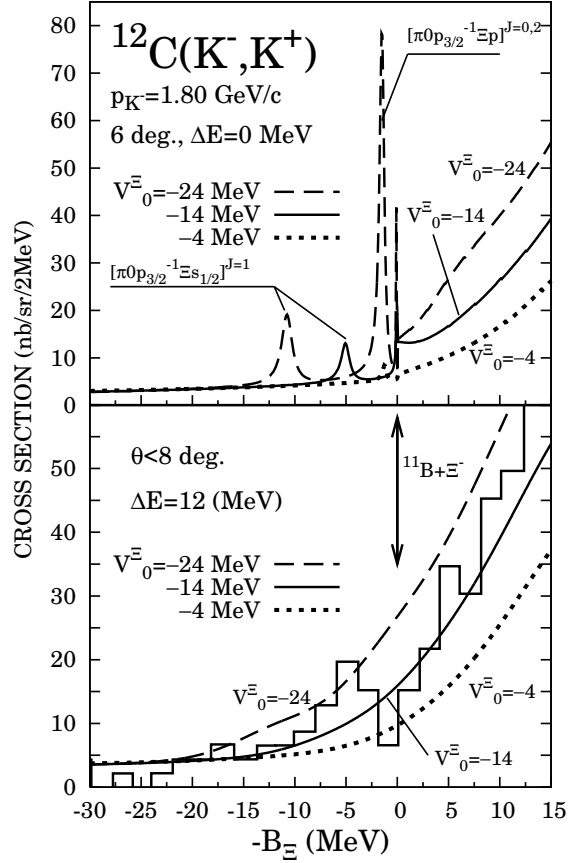


Fig. 3. Potential depth dependence of the Ξ^- -hypernuclear production spectra in the bound state region at $p_{K^-} = 1.80 \text{ GeV}/c$ and $\theta \leq 8 \text{ deg.}$ on ^{12}C without (with) the experimental resolution (upper/lower panel). Dotted, solid and dashed lines show the results with Ξ^- -nucleus potential depths of 24, 14 and 4 MeV, respectively. Experimental data are taken from Ref. [4].

ergies, then there is a possibility that we can determine the potential depth as discussed in Refs. [3]. In Fig. 3, we show the results of the potential depth dependence of the calculated Ξ^- production spectrum on ^{12}C target at $p_{K^-} = 1.80 \text{ GeV}/c$ multiplied by the factors described above in comparison with data [3].

Ikeda *et al.* evaluated the width of Ξ^- hypernuclear states ($^{11}\text{B} + \Xi^-$) to possible double Λ states based on the Nijmegen model D potential as 1.2 MeV and 0.5 MeV for $[\pi 0 p_{3/2}^{-1} \otimes \Xi s_{1/2}]^{J=1}$ and $[\pi 0 p_{3/2}^{-1} \otimes \Xi p]^{J=0,2}$, respectively [15]. In the upper panel of Fig. 3, we show the ideal Ξ^- production spectra on ^{12}C target without the energy resolution folding. The imaginary part is assumed to be $W_0^- = -1 \text{ MeV}$. These calculated spectra show that the Ξ^- hypernuclear state widths are in good

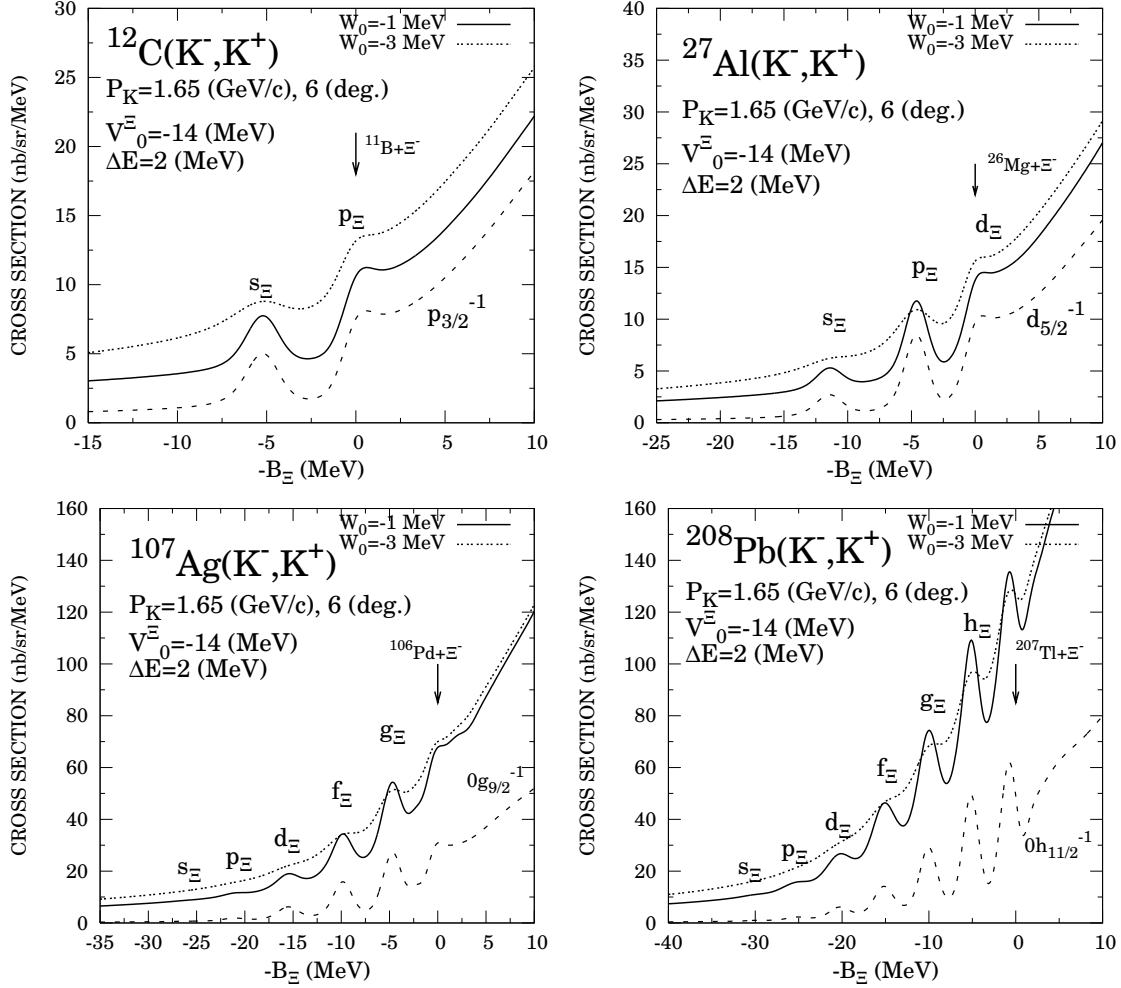


Fig. 4. Ξ^- production spectra at $p_{K^-} = 1.65$ GeV/c and $\theta_{K^+} = 6$ deg. on ^{12}C , ^{27}Al , ^{107}Ag and ^{208}Pb targets expected in the J-PARC experiment. We assume a Woods-Saxon potential with 14 MeV depth, and we show the results with imaginary parts of -1 MeV (solid) and -3 MeV (dotted). Experimental resolution is assumed to be $\Delta E = 2$ MeV (FWHM).

agreements with the estimates in Ref. [15]. In comparison with experimental data, these spectra must be folded using a Gauss function. In the lower panel of Fig. 3, we show the results with an experimental resolution of $\Delta E = 12$ MeV FWHM. Since the experimental resolution is not enough to distinguish the bound state peaks and the statistics is low, we should compare the integrated yield in the bound state region. We find clear potential dependence in the bound state region, and with deep Ξ^- potential ($U_{\Xi} = -24$ MeV) we may find a bump structure at around $-B_{\Xi} \sim -12$ MeV even with this low resolution. Comparison with the data suggests that the potential depth around 14 MeV is preferred in the present treatment, and if the statistics is high enough, it would be possible to determine the

potential depth even with low resolution.

The depth of the Ξ^- -nucleus potential has been already suggested to be around 14 MeV from the analysis of the (K^-, K^+) spectrum in the bound state region [3]. In that analysis, the t -matrix element is evaluated under the frozen nucleon momentum approximation, where the kinematics is given with zero initial nucleon momentum. In the present analysis, while the kinematics in the elementary process and the way to fix the absolute value are different preferred potential depth is similar. This may be due to the fact that the excitation energy dependence of LOFAt is weak and smooth since the covered K^+ momentum range is narrow in the bound state region.

Now we find that Ξ^- -nucleus potential with 14

MeV depth well describes the spectra in the bound state and QF region for light nuclear targets, then it would be valuable to predict the peak structure which would be observed in the future coming J-PARC day-one experiment. Sensitivity of calculated spectra for the Ξ^- -nucleus potential is weak in the QF region because of the high momentum transfer $q \sim 500$ MeV/c, therefore it is difficult to extract precise potential information from the QF region, as shown in Fig. 2

In Fig. 4, we show the calculated K^+ spectra in the bound state region of (K^-, K^+) reactions on ^{12}C , ^{27}Al , ^{107}Ag and ^{208}Pb targets with a potential depth of $V_0^{\Xi} = -14$ MeV, which explains the QF spectra and low resolution spectra in the bound region. We compare the results with $W_0^{\Xi} = -1$ MeV (solid lines) and $W_0^{\Xi} = -3$ MeV (dotted lines). We assume that the experimental resolution of $\Delta E = 2$ MeV would be achieved. We find that bound state peaks are populated selectively due to high momentum transfer ($q \sim 500$ MeV/c) as in the Λ production spectra by (π^+, K^+) reactions ($q \sim 350$ MeV/c), and these peaks can be identified in the high resolution experiment.

In the Green's function method, target nucleon deep hole states are assumed to have large imaginary energies. Therefore, calculated results may be overestimating the spectra around the ground state due to the long Lorentzian tail from the deep hole states having finite contributions in this energy region. This problem will be discussed in the future.

4. Conclusion

We have investigated the Ξ^- -nucleus potential through cascade (Ξ) hypernuclear production spectra by (K^-, K^+) reaction in the Green's function method [7] of the distorted wave impulse approximation (DWIA) with the local optimal Fermi averaging t -matrix (LOFAt) [19]. The calculated spectra are in good agreement with the experimental data for heavy targets. With the multiplicative factor adjusted to fit the spectra on light targets, we find that the calculated spectra well reproduce the observed spectrum [4] in shape and yield with Ξ^- -nucleus potential depth around 14 MeV. This potential depth is consistent with those suggested in previous works [2,3,4].

While the dependence on the potential depth is small in the continuum region, it is clearly distinguished in the bound region. Therefore, it would be

possible to extract the Ξ^- -nucleus potential depth from the production yield in the bound state region when the statistics is high enough. Furthermore, the Ξ^- bound state peak structure can be found in the (K^-, K^+) spectra on light target such as ^{12}C and ^{27}Al , as far as the imaginary part is not very large ($|W_0^{\Xi}| \leq 3$ MeV) and the experimental resolution is improved ($\Delta E \sim 2$ MeV), as expected in the J-PARC experiment. We believe that our prediction would provide useful information in searching for the Ξ^- nuclear bound states at J-PARC.

Acknowledgements

We would like to thank Prof. A. Gal, Prof. T. Harada and Prof. M. Kohno for valuable discussions. This work is supported in part by the Ministry of Education, Science, Sports and Culture, Grant-in-Aid for Scientific Research under the grant numbers, 15540243, 1707005, and 19540252.

References

- [1] C. B. Dover and A. Gal, *Annals Phys.* **146** (1983) 309.
- [2] S. Aoki *et al.*, *Phys. Lett. B* **355** (1995), 45.
- [3] T. Fukuda *et al.*, *Phys. Rev. C* **58** (1998), 1306.
- [4] P. Khaustov *et al.*, *Phys. Rev. C* **61** (2000), 054603.
- [5] T. Iijima *et al.*, *Nucl. Phys. A* **546** (1992), 588.
- [6] E. H. Auerbach, A. J. Baltiz, C. B. Dover, A. Gal, S. H. Kahana, L. Ludeking, and D. J. Millener, *Ann. Phys. (NY)* **148** (1983), 381.
- [7] O. Morimatsu and K. Yazaki, *Nucl. Phys. A* **483** (1988), 493, *ibid* **435** (1985), 727. , M. T. López-Arias, *Nucl. Phys. A* **582** (1995), 440.
- [8] D. V. Bugg *et al.*, *Phys. Rev.* **168** (1968), 1466.
- [9] S. Tadokoro, H. Kobayashi and Y. Akaishi, *Phys. Rev. C* **51** (1995), 2656.
- [10] B. W. Allardyce *et al.*, *Nucl. Phys. A* **209** (1973), 1.
- [11] T. Harada and H. Hirabayashi, *Nucl. Phys. A* **744** (2004), 323, *ibid* **767** (2006), 206, *ibid* **759** (2006), 143.
- [12] Y. Alexander and P. J. Moffa, *Phys. Rev. C* **17** (1978), 676.
- [13] M. Kohno *et al.*, *Prog. Theor. Phys.* **112** (2004), 895. M. Kohno *et al.*, *Phys. Rev. C* **74** (2006), 064613.
- [14] H. Sorge, H. Stoecker and W. Greiner, *Annals Phys.* **192** (1989) 266; A. B. Larionov, W. Cassing, C. Greiner and U. Mosel, *Phys. Rev. C* **62** (2000) 064611; M. Isse *et al.*, *Phys. Rev. C* **72** (2005) 064908 [arXiv:nucl-th/0502058].
- [15] K. Ikeda, T. Fukuda, T. Motoba, M. Takahashi and Y. Yamamoto, *Prog. Theor. Phys.* **91** (1994) 747.
- [16] C. Gobbi, C. B. Dover, A. Gal, *Phys. Rev. C* **50** (1994), 1594.
- [17] Y. Nara *et al.*, *Nucl. Phys. A* **614** (1997), 433.

- [18] S. Hashimoto, M. Kohno, K. Ogata and M. Kawai,
arXiv:nucl-th/0610126.
- [19] H. Maekawa, K. Tsubakihara, A. Ohnishi,
arXiv:nucl-th/0701066.